Cumulative viral load, an indicator of virulence, is controlled by the host's immune response.

Yoh Iwasa (yohiwasa@kyudai.jp)
Kyushu University
Akane Hara
Hokkaido University
Shihomi Ozone
Kwansei Gakuin University

Research Article

Keywords: viral growth rate, cytotoxic T cells, memory T cells, mutation.

Posted Date: May 6th, 2021

DOI: https://doi.org/10.21203/rs.3.rs-483920/v1

MS without SI

Cumulative viral load, an indicator of virulence, is controlled by the host's immune response.

by

[1]Yoh Iwasa, [2]Akane Hara, and [1]Shihomi Ozone

[1]*Department of Biology, Faculty of Science, Kyushu University, 744 Motooka, Nishi-ku, Fukuoka 819-0395, Japan*

[2]*Department of Advanced Transdisciplinary Sciences, Hokkaido University, Sapporo, Hokkaido 060-0810, Japan*

[3]*Department of Bioscience, School of Science and Technology, Kwansei Gakuin University, Gakuen 2-1, Sanda-shi, Hyogo 667-1339, Japan*

corresponding author:

Yoh Iwasa
Department of Biology,
Kyushu University,
744 Motooka, Nishi-ku,
Fukuoka 819-0035, Japan
email: yohiwasa@kyudai.jp
phone: +81-92-(0)80-5268-2641
coauthors emails: hara.akane32a@gmail.com; shmtrlaw@gmail.com

(submitted to *Scientific Reports*, May 1, 2021)

Abstract (195 words)

A viral strain may infect a host, proliferate rapidly, become controlled by immune reactions, and eventually be eliminated from the body. The virulence, or the magnitude of harm to the host due to infection, depends on the abundance and duration of the viral strain in the body, and the importance of the damaged tissue of the host. In this study, we investigated how the cumulative viral load (time-integral of the number of infected cells) depends on various factors, such as the viral growth rate, the effectiveness of immune cells to kill infected cells, speed of immune activation, formation of memory cells, and longevity of immune cells. In addition, viruses may produce a mutant with different antigen types, escape the immune reaction targeting the original type, and inflate virulence. We derived four simple formulas for the cumulative viral load that holds in different parameter regions. We analyzed the sensitivity of the cumulative viral load to the parameters in the model. Additionally, we discussed the reported correlation between virulence and molecular evolution rate. We conclude that viral virulence can be mitigated by enhancing the speed and effectiveness of immune reactions and by reducing the viral growth rate.

key words: viral growth rate; cytotoxic T cells; memory T cells; mutation.

1. Introduction

A virus is a particle containing nucleic acids and proteins packed within the coat protein shell. Viruses proliferate, exploiting the metabolic system of the host cells. It has its own genome, either DNA or RNA. Viruses have characteristics intermediate between living system and non-living systems and can act as pathogens in the host.

Viruses invading a host body are digested by antigen-presenting cells, which activate naive T cells that are reactive to specific antigens of the virus. This results in the proliferation of active cytotoxic T cells (i.e. killer T cells) that kill cells infected by the virus and reduces the number of infected cells. In addition, a fraction of the activated naive T cells become memory T cells that have a long life. Memory T cells maintain the level of cytotoxic T cells and prepare for re-infection with the same virus in the future. We consider the time integral of the viral abundance in the body until the virus is cleared from the body and refer to it as the "cumulative viral load" [1,2,3]. Virulence, or harm to host health, would increase with the cumulative viral load.

If the virus mutates to a type that has a different antigen specificity, the immune reactions targeting the original type cannot suppress the mutant strain. Hence the mutant strain escapes immune surveillance. To suppress the mutant viral strain, the host immune system needs to develop cytotoxic T cells that are reactive to the new antigen type. The host would suffer additional harm until the second strain is eliminated. If one or more additional mutants of different antigen types are created, they may cause a further increase in the cumulative viral load. We can evaluate the total number of cells infected by the viral strain(s), including the initial type and all of its descendants.

Many models for the immune reactions in the body consider the number of cells infected by the viral strain and the immune reactions represented by cytotoxic T cells [4]. They describe the initial rapid increase in virus abundance followed by the decline as a result of immune reactions. However, the virus cannot be eliminated from the body because in the absence of viral antigens the level of immune reaction (i.e., cytotoxic T cell number) decreases due to their mortality, resulting in the persistence of the virus within the body at low levels [5,6]. In these models, cumulative viral load cannot be used to evaluate virulence, because the time integral of the number of infected cells will be infinitely large.

In the present study, we adopted the model studied by Hara and Iwasa [7], in which the number of memory T cells is considered. Memory T cells remain at a positive level because of their long life and continue to produce active cytotoxic T cells, which eventually eliminate the virus form the body. In this paper, we represent the viral abundance based on the number of infected cells, rather than the number of viral particles [4]. We first consider the dynamics of the numbers of infected cells $V(t)$, cytotoxic T cells $H(t)$, and memory T cells $M(t)$. We then calculate the cumulative viral load, defined as the time integral of the number of infected cells $\int_0^\infty V(t)dt$, when the initial dose of viral number is very small.

To evaluate the parameter dependence of the cumulative viral load, $\int_0^\infty V(t)dt$, we first reduce the number of parameters in the model from six to two (α and β) by rescaling three variables and one-time parameter properly. The contour map of the cumulative viral load in the reduced dynamics with rescaled variables exhibits a characteristic simple dependence on α and β in four different regions. By converging

this result to the original model, we have simplified formulas for the sensitivity of the cumulative viral load to six parameters. We examine the total cumulative viral load when mutations may produce strains with different antigen types that escape immune surveillance. Additionally, we discuss the correlation between the rate of molecular evolution and virulence among several viral strains that infect rainbow trout [8].

2. Model

We denote the number of infected cells by V, the number of cytotoxic T cells that attack the infected cells by H, and the number of memory T cells by M. Initially, a newly infecting virus proliferates exponentially in the host. However, the virus is checked by immune reactions and eventually eliminated from the host. In epidemiology and theoretical immunology, the time-integral of the viral abundance in the host body, referred to as "cumulative viral load," is adopted as a good indicator of virulence and prognosis [1,2,3]. In this paper, we define the cumulative viral load as the number of infected cells integrated by the time parameter.

To evaluate the importance of different processes controlling virulence by their effects on the cumulative viral load, we need to adopt a mathematical model describing the temporal peak abundance of the virus population, followed by a decline in abundance and by clearance from the body in the end. However, many models for viral dynamics end up with a stable state with a low but positive abundance of pathogens remaining in the body (persistent infection), instead of virus clearance after a temporal infection [4,9]. In these models, the cumulative viral load is infinitely large and cannot be used as a basis for comparing different processes. To discuss the eventual viral clearance, immune cells with a long lifetime must be considered [5,6].

In the present study, we consider memory T cells that have a very long life. For simplicity of analysis, we neglect the mortality of memory T cells, as assumed in [7]. The dynamics are given as:

$$\frac{dV}{dt} = rV - bHV, \tag{1a}$$

$$\frac{dH}{dt} = aV + qM - cH, \tag{1b}$$

$$\frac{dM}{dt} = qV. \tag{1c}$$

Eq. (1a) indicates the dynamics of the number of infected cells in a host. We assume that in the absence of an immune reaction, they proliferate exponentially with a growth rate r. Their increase is checked by the immune activity of cytotoxic T cells H. The number of infected cells killed by cytotoxic T cells is proportional to the product of infected cell abundance and cytotoxic cell abundance, where b is the proportionality coefficient, indicating the effectiveness of the immune reaction.

Eq. (1b) indicates the dynamics of cytotoxic T cells that are reactive to the viral antigens. They are produced from naive T cells which remain inactive if there are no antigens within the body. In the presence of a virus, they would mature and become active cytotoxic T cells, at a rate proportional to viral abundance with proportionality coefficient a, as indicated by the first term on the right-hand side of Eq. (1b). The second term on the right-hand side indicates the supply of cytotoxic T cells from memory T cells M. The third term of Eq. (1b) indicates the loss of cytotoxic T cells due to daily mortality c. The mean longevity of the cytotoxic T cells is $1/c$.

Eq. (1c) indicates the dynamics of memory T cells that are reactive to the viral antigens. We assume that a small fraction of these cells become memory T cells with a long life. Hence, their number increases at a rate proportional to the viral abundance V,

144 with proportionality coefficient u. We here neglect the mortality of memory T cells, as
145 assumed in [7].
146 We consider a situation in which the initial dose of the viral infection is very
147 small, indicated by a small and positive number ε. Hence, the initial condition of Eq.
148 (1) is
149 $V(0) = \varepsilon,\ H(0) = 0$, and $M(0) = 0$. (2)
150 The trajectory and the final state depend on the value of ε. In this study, we are
151 interested in the limit when ε is very small ($\varepsilon \to 0$).
152
153 *2.1. Cumulative viral load of a single viral strain with the same antigen type*
154 Fig. 1 illustrates a typical time course of viral infection, represented by Eq. (1).
155 At time 0, the host is infected by a small dose of the virus. The viral abundance
156 increases rapidly and is checked by immune reactions, represented by cytotoxic T cells,
157 and eliminated from the host body. The abundance of cytotoxic T cells increases, shows
158 a peak abundance, and starts declining slowly after the clearance of the virus from the
159 body. The abundance of memory T cells increases while some viruses exist in the host
160 body, but stops increasing after the virus clearance.
161 We assume that the cumulative viral load, defined as the time integral of the
162 number of infected cells, would be a good indicator of virulence and the magnitude of
163 harm to host health due to the infection. Here we denote it by φ:
164 $\varphi = \int_0^\infty V(t)dt.$ (3a)
165 In Fig. 1(c), this is illustrated as the area under curve $V(t)$. The amount of harm due to
166 viral infection is proportional to φ with the coefficient of proportionality h_0.
167 [harm due to the pathogen infection] $= h_0\varphi$ (3b)

168 h_0 indicates the importance of the tissue attacked by the virus. If a mutation produces a
169 viral strain that escapes immune control, the host immune system must activate immune
170 cells with the mutant's antigen specificity, making the virulence even larger than Eq.
171 (3b). We will discuss this effect in a later section.
172
173 **3. Four regions of simple parameter dependence**
174 We first attempt to estimate φ, given by Eq. (3a).
175
176 *3.1 Reduced dynamics*
177 The model Eq. (1) includes six parameters: r, b, a, q, c, and u. We
178 introduce the following four variables: $\bar{V} = k_v V$, $\bar{H} = k_h H$, $\bar{M} = k_m M$, and $\tau = k_t t$.
179 By choosing k_v, k_h, k_m, and k_t in a suitable manner, we obtain the dynamics of
180 $\bar{V}(\tau)$, $\bar{H}(\tau)$, and $\bar{M}(\tau)$, which include only two parameters: α and β, as follows:
181 $$\frac{d\bar{V}}{d\tau} = \bar{V} - \bar{H}\bar{V}, \quad (4a)$$
182 $$\frac{d\bar{H}}{d\tau} = \alpha\bar{V} + \bar{M} - \beta\bar{H}, \quad (4b)$$
183 $$\frac{d\bar{M}}{d\tau} = \bar{V}, \quad (4c)$$
184 where
185 $$\alpha = \frac{ar}{qu} \text{ and } \beta = \frac{c}{r}. \quad (4d)$$
186 For the derivation, see Appendix A in Supplementary Information.
187 In the initial condition, $\bar{V}(0)$ is a very small positive quantity, and the other
188 two values are zero: $\bar{H}(0) = \bar{M}(0) = 0$. We can represent the integral in Eq. (3a) as
189 follows:

$$\varphi = \int_0^\infty V(t)dt = \frac{r^2}{qub}\int_0^\infty \bar{V}(\tau)d\tau. \quad (5a)$$

Now, we focus on the time integral on the right-hand side of Eq. (5a). It is

$$\psi(\alpha,\beta) = \int_0^\infty \bar{V}(\tau)d\tau = \bar{M}(\infty), \quad (5b)$$

where the last equality is derived from Eq. (4c) and $\bar{M}(0) = 0$. Because the dynamics in Eq. (4) include only α and β, Eq. (5b) is a function of these two quantities.

Fig. 2 illustrates the contour map of $\psi(\alpha,\beta)$ where the horizontal axis and vertical axis are for β and α, respectively, both expressed on a logarithmic scale. The values were obtained by numerical integration. $\psi(\alpha,\beta)$ is large when α is small and β is large, and it is small when α is large and β is small. In several locations, contours are parallel to each other, and they are vertical in some regions but horizontal in other regions.

This observation can be mathematically explained. In Appendix B of the Supplementary Information, we derived four simple formulas for $\psi(\alpha,\beta)$ that hold in different parameter regions in the (α,β)-plane. Results are:

[I] When α is large and β is not small, $\psi(\alpha,\beta) = \beta$, (6a)

[II] When α is small and β is large, $\psi(\alpha,\beta) = 2\beta$, (6b)

[III] When β is very small and α is large, $\psi(\alpha,\beta) = \frac{2}{\alpha}$, (6c)

[IV] When both α and β are small, $\psi(\alpha,\beta) = 1.306$. (6d)

The last value was numerically calculated for $\alpha = \beta = 0$. Please see Appendix B for the derivation of these limiting behaviors and the conditions under which they are valid.

Fig. 3(a) illustrates how $\psi(\alpha,\beta)$ depends on α, as shown on a logarithmic scale. Different curves were obtained for different values of β. In contrast, Fig. 3(b) shows $\psi(\alpha,\beta)$, and the horizontal axis is β. Different curves were obtained for

different values of α. The predictions of the four formulas in Eqs. (6a)-(6d) are indicated by thick straight line segments with Roman numbers ([I], [II], [III], and [IV]) distinguishing the four regions. From these figures, we can conclude that the predictions of the four formulas are accurate in their respective regions, and that ψ for intermediate parameter values between different regions connects smoothly between the predictions of the formulas.

3.2 Cumulative viral load in four parameter regions

Eq. (5) indicates that the cumulative viral load φ is the product of $\psi(\alpha, \beta)$ and the factor r^2/qub. By combining this with the four approximate formulas in Eq. (6), we have formulas for the cumulative viral load φ, in these four different regions:

[I] When α is large and β is not small, $\varphi = \frac{rc}{qub}$. (7a)

[II] When α is small and β is large, $\varphi = \frac{2rc}{qub}$. (7b)

[III] When β is very small and α is large, $\varphi = \frac{2r}{ab}$. (7c)

[IV] When both α and β are small, $\varphi = 1.306\frac{r^2}{qub}$. (7d)

We can see that the cumulative viral load φ follows formulas different between parameter regions, and hence its parameter dependence varies with α and β.

From the four formulas in Eq. (7), we can see that the cumulative viral load should increase with the viral growth rate r, and decrease with the effectiveness of the immune cells b, in all four regions.

However, tor other rate constants, the dependence may differ between the regions. The cumulative viral load decreases with the mortality of cytotoxic T cells c when β is large, but it is independent of c when β is small. a is the rate of increase

236 of the cytotoxic T cells H directly due to the virus, and q and u are the rate of
237 increase of H indirectly via memory T cells M. The cumulative viral load φ
238 decreases with q and u but not with a, in regions [I], [II] and [IV]; however, φ
239 decreases with a but not with q or u in region [III].
240 Pathogenic viral strains causing infectious diseases probably have a doubling
241 time shorter than the longevity of cytotoxic T cells. If so, $\beta = c/r$ is likely to be
242 smaller than 1. In this parameter region, we have three regions exhibiting different
243 dependences on $\alpha = ar/qu$. Table 1 shows these three cases, in which different
244 approximate formulas of cumulative viral load hold. In all three regions, the cumulative
245 viral load increases with r, decreases with b, but is independent of c. For other
246 parameters (a, q, and u), the dependence varies between regions, depending on $\alpha =$
247 ar/qu. α indicates the relative importance of direct enhancement of cytotoxic T cells
248 (a) and indirect enhancement via memory T cells (q and u).
249 In contrast, if the virus grows very slowly compared to the turnover time for
250 cytotoxic T cells ($\beta = c/r > 1$), the parameter dependence of the cumulative viral load
251 is simple: it is proportional to rc/qub, hence, the cumulative viral load increases with
252 growth rate r and mortality of cytotoxic T cells c and decreases with the effectiveness
253 of cytotoxic T cells in removing virus b, and the effectiveness of viral activation of
254 cytotoxic T cells via memory T cells (q and u). Interestingly, the cumulative viral load
255 is independent of a, the rate of direct activation of cytotoxic T cells.
256
257 *3.3 Sensitivity to intermediate parameter values*
258 The parameter sensitivity of the cumulative viral load is represented in terms of
259 elasticity; the elasticity of φ for parameter k is $c_k = \partial ln\varphi/\partial lnk = (k/\varphi)(\partial\varphi/\partial k)$.

This quantity is useful because it is independent of the choice of "unit" of each quantity, and has been widely used to represent parameter sensitivity in economics and ecology [10,11]. In this study, we adopted elasticity to represent the parameter sensitivity of the cumulative viral load.

We often do not know realistic values of rate parameters accurately, such as viral proliferation rate, immune reaction speed, the effectiveness of cytotoxic T cells and the responses of memory T cells. We would be happy if parameters happen to be one of the four regions in which simple formulas are available. However, realistic parameters may have values between different regions. To understand the effectiveness of different therapeutic treatments, we need to know the parameter sensitivity or elasticity, in these intermediate regions.

We performed a sensitivity analysis of the cumulative viral load $\varphi = \int_0^\infty V(t)dt$ numerically. We first chose a standard parameter set and calculated φ for points around the standard parameter set. Then using the multivariate analysis, we calculated the regression of the logarithm of φ, on the logarithmic values of the parameters:

$$ln\varphi = c_0 + c_r lnr + c_c lnc + c_a lna + c_q lnq + c_u lnu + c_b lnb + [\text{noises}], \quad (8)$$

where we chose the natural logarithm (i.e., the base is Napier's constant). The coefficients c_r, c_c, c_a, c_q, c_u, and c_b are the elasticities of φ for the respective parameters.

The elasticity of φ for the parameters depends on the standard parameter set, specifically on two quantities: $\alpha = ar/qu$ and $\beta = c/r$. To examine the sensitivity at different standard values, we examined the elasticity of φ at $49(= 7 \times 7)$ combinations of α and β (α and β are chosen from $1/64$, $1/16$, $1/4, 1, 4, 16$,

284 64). For each pair of α and β, we calculated the elasticity of φ for six parameters (r,
285 c, a, q, u, and b). The method used to calculate the elasticity numerically is
286 explained in Appendix C of the Supplementary Information.
287 Figs. 4(a)-4(f) illustrate the value of the regression coefficients, c_r, c_c, c_a,
288 c_q, c_u, and c_b, respectively, obtained numerically near the standard values α and β,
289 which are indicated in two axes. Main results are as follows:
290 First, in the four regions, [I], [II], [III], and [IV], as discussed in the previous
291 section, the regression coefficients were close to the elasticity values expected from
292 simple formulas, Eqs. (7a)-(7d).
293 Second, in the region connecting these four regions, regression coefficients
294 (i.e., elasticities) may differ from the value inferred by interpolation between nearby
295 regions where four formulas hold. For example, when β is large ($\beta \geq 16$), the
296 regression coefficient of parameter a was close to 0 ($c_a \approx 0$) for both very large α
297 and very small α. However, for intermediate values of α, c_a was smaller than 0
298 ($c_a \approx -0.17$ when $\alpha = 1,4$ and $\beta = 4,16,64$ in Fig. 4(c)). c_r was close to 1 for
299 very large α and for very small α, but it was smaller than 1 for intermediate values of
300 α ($c_r \approx 0.83$ when $\alpha = 1,4$ and $\beta = 4,16,64$ in Fig. 4(a)). Similarly, both c_q and
301 c_u were close to -1 for both very large α and very small α, but were higher than
302 -1 for intermediate α ($c_q \approx c_u \approx -0.83$ when $\alpha = 1,4$ and $\beta = 4,16,64$ in Fig.
303 4(d) and 4(e)). Hence, the regression coefficients, c_a, c_r, c_q and c_u exhibit a non-
304 monotonic dependence on α, as is illustrated clearly in Fig. S1 in Appendix C of
305 Supplementary Information.
306 Third, the sensitivity for q and that for u were the same for all the values of
307 α and β. This is plausible because the time integral of the viral abundance is given by

$\varphi = (r^2/qub) \cdot \psi(ar/qu, c/r)$, where q and u appear as product qu.

4. Viral load enhanced by mutations changing antigen type

Proliferation of the virus provides an opportunity for novel mutations to occur. During an episode of proliferation of a single strain, the total number of newly infected cells is $r\int_0^\infty V(t)dt$, the product of viral growth rate and the number of infected cells integrated over time. The expected number of mutants produced from a single infected cell is this quantity multiplied by the rate of mutations changing antigen-type m_A, which is measured as the fraction of mutant virus particles of different antigen types among those produced from a single infected cell. We denote this by p.

$$p = m_A r\int_0^\infty V(t)dt = m_A r\varphi. \quad (9)$$

For simplicity, we assume that all novel mutations have different antigen types. The number of those mutations follows a Poisson distribution with mean p. Each of these mutations may produce novel mutations, the number of which, in turn, follows a Poisson distribution with mean p.

Fig. 5 illustrates the case in which a single viral strain produced three novel mutant strains that differ in antigen types. We call them first-generation strains ($X_1 = 3$). The expected number of first-generation strains is p. These three strains produced two second-generation strains ($X_2 = 2$). The expected number of second-generation strains is p^2. Each of these two-step mutants may produce three-step mutants. The expected total number of these three-step mutants is p^3. If we continue these calculations, the expected number of total mutant strains starting from a single initial strain is $1 + p + p^2 + p^3 + p^4 + \ldots = \frac{1}{1-p}$.

The total cumulative viral load in the presence of mutations generating novel antigen types is the one without mutations φ multiplied by this factor:

$$[\text{total cumulative viral load}] = \varphi \frac{1}{1-m_A r \varphi}. \quad (10)$$

The virulence of an infection event should increase with the time-integral of cumulative viral load, $\varphi = \int_0^\infty V(t)dt$, which is the quantity evaluated in this study. However, there is an additional effect of $m_A r$ that further inflates the cumulative viral load. If the virulence is the total cumulative viral load multiplied by h_0, the virulence increases nonlinearly with φ, as shown in Eq. (10). The opportunity to produce strains of novel antigen types strengthens the importance of φ.

5. Discussion

In this study, we studied the cumulative viral load of viral strains, assuming that those growing to a large number and staying longer within the host tend to cause more harm to the host. A strain is more virulent if it grows very fast before the immune system starts to control it, if the strain does not cause a strong response to the immune system, or if the strain mutates to antigen type different from the original ones and escapes immune surveillance. However, the virulence of a strain must additionally depend on the importance of the tissue attacked by the virus. Infection with a virus might be fatal to the host if the virus breaks down the tissue that is critical to the host's health, even if the abundance of the virus may not be very large. We represented this effect as the coefficient h_0, which depends on the biology of the virus and the host.

5.1 Four parameter regions

354 The time-integral of the viral load, φ, has mathematical properties worthy of
355 detailed examination. After rescaling variables, it becomes a quantity ψ depending on
356 two combinations of variables: $\alpha = ar/qu$ and $\beta = c/r$. As shown in Fig. 2, the four
357 parameter regions exhibit simple parameter dependence. We derived four explicit
358 formulas that were quite accurate, as shown in Fig. 3.
359 There four parameter regions exhibit different characteristic parameter
360 dependence of cumulative viral load φ. φ increases with r in all four regions, but φ
361 increases in proportion to r in [I], [II], and [IV], while φ increases in proportion to
362 r^2 in [III]. φ decreases with b in all four regions. φ increases with c both in [I]
363 and [II], but it is independent in [III] and [IV].
364 Interestingly, the dependence of φ on the direct activation of cytotoxic T cells
365 a and the indirect activation via memory T cells q and u differ between regions In
366 regions [I], [II], and [IV], φ decreases with q and u, but it is independent of a; In
367 contrast, in region [III], φ decreases with a, but it is independent of q or u. Hence,
368 the relative effectiveness of direct activation of cytotoxic T cells and indirect activation
369 via memory T cells in suppressing cumulative viral load may differ between the
370 standard values.
371 In the boundary between these four regions, we often observed smooth and
372 monotonic changes between the regions. However, at the boundary between [I] and [II]
373 (i.e. $1 \leq \alpha \leq 4$ and $\beta \geq 1$), we observed a significant and characteristic deviation of
374 parameter dependence, represented as elasticity (see Fig. S1 in Supplementary
375 Information).
376 Most importantly, we cannot neglect the presence of memory T cells to
377 evaluate cumulative viral load. This is because, without memory T cells (i.e., either

$q = 0$ or $u = 0$), cytotoxic T cells cannot eliminate the virus-infected cells, making the cumulative viral load infinitely large.

5.2 Correlation between virulence and the rate of molecular evolution

Reports show that the rate of molecular evolution is faster for more virulent strains than less virulent ones. For example, IPNV (genus *Auabiruavirus*, family Birnaviridea) is a pathogen of rainbow trout. It was reported in the late 1970s for the first time in an aquaculture facility in Italy, and eventually became endemic. Its prevalence at the farm level was approximately 40 percent, and the estimated mortality of juveniles was 10-30 percent. IPNV strains with low virulence tend to have a slower rate of genomic replication and a slower rate of molecular evolution [8].

The rate of molecular evolution would increase with the total number of virus replications made in the population, which is related to the following products:

$$\begin{bmatrix}\text{virus abundance}\\ \text{within a host}\end{bmatrix} \times \begin{bmatrix}\text{number of infected}\\ \text{individuals}\\ \text{per pandemic event}\end{bmatrix} \times \begin{bmatrix}\text{frequency of pandemic}\\ \text{events per year}\end{bmatrix}.$$

The first factor is the cumulative viral load and is likely to be correlated with the virulence. The second factor, the number of infected individuals per pandemic event, also depends on the rate at which the virus would be taken in the body of the susceptible host and successfully infected the host, and the number of viral particles released from an infected host, which may be correlated with the cumulative viral load. However, it additionally depends on other factors, such as the contact rate between host individuals and the host population structure. The third factor, the frequency of pandemics, may or may not be correlated with virulence. Taken together, there are many ways in which virulence is correlated with the rate of molecular evolution, although we need to model

401 how the number of infected individuals is related to the virus abundance within an
402 infected host.
403 In this section, we discusse the effect of a large cumulative viral load, an
404 important factor of virulence, on the rate of molecular evolution, which is a question
405 that has not been discussed intensively. In contrast, the evolution of virulence levels for
406 pathogens has been the focus of many theoretical studies for more than two decades [12,
407 13, 14, 15, 16, 17, 18]. A traditional argument was that the virus that recently became to
408 attacked a host species may be very virulent, but they tend to evolve more benign,
409 because killing the host quickly would reduce the chance of transmission to susceptible
410 hosts and is disadvantageous to the virus. However, the virulence may not decrease in
411 evolution if a higher transmission rate is accompanied by a larger virus abundance,
412 which inevitably causes the infected host to have a shorter life [15]. In addition, the
413 spatial structure of the host population may produce an evolution toward enhanced
414 virulence [19,20].
415
416 *5.3 Implications to the chemotherapy of virus*.
417 The parameter dependence of the cumulative viral load would be useful for
418 understanding the variation in virulence among strains and for designing drug therapy.
419 The analyses of parameter sensitivity (or elasticity) suggest effective options for
420 reducing the virulence of viral pathogens as follows:
421 When the longevity of the cytotoxic T cells is longer than the doubling time of
422 viral proliferation, we have the following three options:
423 (1) Reduce the growth rate of the viral strain (decrease r).
424 (2) Enhance the effectiveness of the immune system in killing the virus (increase b).

(3) Facilitate the activation of the immune system in response to viral antigens (increase a).

In contrast, when the longevity of the cytotoxic T cells is shorter than the doubling time of the viral strain, we have (1) and (2) again. However (3) must be replaced by the following

(3') Facilitate the formation of memory T cells and the production of cytotoxic T cells by the memory T cells (increase u and q).

For the proliferation of viruses within a host, viruses need to perform several key processes successfully, such as infecting target cells, forming mature viral particles, releasing free viral particles out of the infected cells and/or transferring the genome to another target cell on the opportunity of cell-to-cell contact. Many drugs aim to slow down the proliferation rate of virus r, by intervening in any of these steps [22,23]. The results of this study suggest that facilitating immune reactions is equally important. Pathogens might be equipped with mechanisms to suppress checking the immune reaction, similar to cancer cells, which have mechanisms to suppress immune reactions by inducing regulatory T cells [23,24]. The study in this paper shows that the rate of immune activation by the presence of infected cells a, the longevity of immune cells $1/c$, the effectiveness of the immune cells in killing infected cells b, the rate of formation of memory cells q, and the effectiveness of memory cells to maintain the level of immune cells u reduce the cumulative vial load, thereby mitigating the virulence. Interestingly, their effectiveness differed between the parameter ranges as shown by sensitivity analyses (Table 1 and Fig. 4), which could be useful in designing immunotherapy for viral pathogens.

Acknowledgements

We thank the following people for their useful comments: Y. Fujita, S.Y. Guo, S. Hishida, Y. Kanayama, K. Kiriyama, M. Kishioka, R. Kobayashi, H. Matsuo, Y. Michibata, R. Nakai, K. Nakanishi, A. Nishiura, R. Ohashi, and A. Shinohara.

Author contributions

Y.I., A.H., and S.O. designed the study, performed the study, and wrote the paper.

Additional information

Competing interests

The authors declare no competing interests.

Data availability

Data sharing does not apply to this article, as no datasets were generated or analyzed during this study.

Supplementary information

See the attached file.

References

[1] Marconi, V.C., G. Grandits, J.F. Okulicz, G. Wortmann, A. Ganesan, N. Crum-Cianflone, M. Polis, M. Landrum, M.J. Dolan, S.K. Ahuja, B. Agan, H. Kulkarni, the Infectious Disease Clinical Research Program (IDCRP) HIV Working Group. 2011. Cumulative viral load and virology: decay patterns after antiretroviral therapy in HIV-infected subjects influence CD4 recover and AIDS. PLOS ONE 6: e17956.

[2] Sempa, J.B., J. Dushoff, M. J. Daniels, B.Castelnuovo, A. N. Kiragga, M. Nieuwoudt, & S. E. Bellan. 2016. Reevaluating cumulative HIV-1 viral load as a prognostic predictor: predicting opportunistic infection incidence and mortality in a Ugandan cohort. American Journal of Epidemiology. 184, 67–77.

[3] Sempa, J.B., T. M. Rossouw, E. Lesaffre, & M. Nieuwoudt. 2019. Cumulative viral load as a predictor of CD4+ T-cell response to antiretroviral therapy using Bayesian statistical models PLOS ONE 14(11): e0224723.

[4] Nowak, M.A. and May, R.M. 2000 "Virus dynamics: mathematical principles of immunology and virology." theoretical immunology" Oxford University Press. pp.237.

[5] Wodarz, D., R.M. May, & M.A. Nowak 2000. The role of antigen-independent persistence of memory cytotoxic T lymphocites. International Immunology 12:467-477.

[6] Wodarz, D. & M.A. Nowak. 2000. CD8 memory, immunodominance, and antigenic escape. European Journal of Immunology 30: 2704-2712.

493 [7] Hara, A. and Y. Iwasa. 2020. Autoimmune diseases initiated by a pathogen
494 infection: mathematical modeling. *J. Theor. Biol.* 498: 110296 (Open Access)
495 https://www.sciencedirect.com/science/article/pii/S002251932030151X
496 [8] Panzarin, V. E C Holmes, M. Abbadi, G. Zamperin, R. Quartesan, A. Milani, A.
497 Schivo, L. Bille, M.D. Pozza, I. Monne, & A. Toffan 2018. Low evolutionary
498 rate of infectious pancreatic necrosis virus (IPNV) in Italy is associated with
499 reduced virulence in trout. Virus Evolution 4(2):vey019.
500 [9] Shudo, E., & Y. Iwasa. 2004 Dynamic optimization of defense, immune memory,
501 and post-infection pathogen levels in mammals. Journal of Theoretical Biology
502 228:17-29.
503 [10] Acemoglu, D. 2002. Directed technical change. Review of Economic Studies
504 69:781-809.
505 [11] de Kroon, H., A. Plaisier, J. van Groenendaef, & H. Caswell. 1986. Elasticity: the
506 relative contribution of demographic parameters to population growth rate.
507 Ecology 67: 1427-1431.
508 [12] May, R., Anderson, R. 1979. Population biology of infectious diseases: Part II.
509 *Nature* 280, 455–461. https://doi.org/10.1038/280455a0
510 [13] Ewald, P.W. 1993. The evolution of virulence. Scientific American 268: 86-##
511 [14] Ewald, P.W. 1995 The evolution of virulence -- a unifying link between
512 parasitology and ecology. J. Parasitology 81: 659-669.
513 [15] Lenski, R.E. & May R.M. 1994. The evolution of virulence in parasites and
514 pathogens -- reconciliation of 2 competing hypotheses. Journal of Theoretical
515 Biology 169:253-265.

516 [16] Nowak, M.A. and R.M. May. 1994. Superinfection and the evolution of parasite
517 virulence. Proceedings of the Royal Soc. Ser B. 255:81-89.
518 [17] Antia, R., Levin, B.R. and May, R.M. 1994. Within-host population dynamics and
519 the evolution and maintenance of microparasite virulence. American Naturalist
520 144: 457-472.
521 [18] Sasaki, A. 2000. Host-parasite coevolution in a multilocus gene-for-gene system.
522 Proceedings of the Royal Society B 267: 2183-2188.
523 [19] Boots, M. & Sasaki, A. 1999. 'Small worlds' and the evolution of virulence:
524 infection occurs locally and at a distance. Proceedings of Royal Soc. B
525 266:1933-19
526 [20] Boots, M., Hudson, P.J., Sasaki, A. 2004. Large shifts in pathogen virulence relate
527 to host population structure. Science 303: 842-844.
528 [21] Bartenschlager, R., V. Lohmann, and F. Penin. 2013. The molecular and structural
529 basis of advanced antiviral therapy for hepatitis C virus infection. Nature
530 Review Microbiology. 11: 482-496.
531 [22] Eastman, R.T., J. S. Roth, K. R. Brimacombe, A. Simeonov, M. Shen, S. Patnaik,
532 and M. D. Hall. 2020. Remdesivir: A review of Its discovery and development
533 leading to emergency use authorization for treatment of COVID-19. ACS Cent.
534 Sci. 6: 672–683.
535 [23] Sakaguchi, S. 2004. Naturally arising CD4(+) regulatory T cells for
536 immunologic self-tolerance and negative control of immune responses
537 Annual Review of Immunology 22: 531-562.
538 [24] Nishikawa, H. and Sakaguchi S. 2010. Regulatory T cells in tumor immunity.
539 International Journal of Cancer 127: 759-767.

Table 1 Directions of change in φ, the cumulative viral load, when each of six parameters increases by a small amount. Up, down, and horizontal arrows indicate an increase, decrease, and no change, respectively. Depending on $\alpha = ar/qu$, three different formulas hold, and parameter dependence differs between them. Here we show the results when $\beta = c/r$ is small. See text for explanations.

	$\frac{ar}{qu} < 1$	$\frac{ar}{qu} > 1$	$\frac{ar}{qu} \gg 1$
formulas	$\frac{1.306r^2}{qub}$	$\frac{2r}{ab}$	$\frac{2rc}{qub}$
r	↑↑	↑	↑
b	↓	↓	↓
c	→	→	↑
a	→	↓	→
q, u	↓	→	↓

Captions to figures

Figure 1 Time course of the model. (a) $H(t)$: cytotoxic T cells; (b) $M(t)$: memory T cells; (c) $V(t)$: viral abundance. The size of the shaded area is the time-integral of viral abundance, φ. Horizontal axis is time t. Parameters are: $r = 0.1$, $c = 0.05$, $a = 0.1$, $q = 0.01$, $u = 0.1$, and $b = 0.1$.

Figure 2 Contour map of $\psi(\alpha, \beta)$. ψ is given by Eq. (5b). It is calculated numerically for (α, β), where $\frac{1}{128} \leq \alpha \leq 128$ and $\frac{1}{128} \leq \beta \leq 128$. Horizontal and vertical axis are β and α. Numbers on contours indicate ψ levels.

Figure 3 Dependence of $\psi(\alpha, \beta)$ on α and β. (a) Dependence of ψ on α. Horizontal axis indicates α. Different curves are for different values of β. (b) Dependence of ψ on β. Horizontal axis indicates β. Different curves are for different values of α. Thick solid line segments indicate the values predicted by simple formulas, Eqs. (6a)-(6d). Roman numbers distinguish respective regions.

Figure 4 Elasticity of φ for six parameters. They are obtained by regression analysis performed around the standard parameter sets. Numbers in boxes are: (a) c_r; (b) c_c; (c) c_a; (d) c_q; (e) c_u; and (f) c_b. The positive and negative level coefficients are represented in red and blue, respectively. These figures illustrate how the elasticity depends on the choice of the standard parameter sets, chosen from $7 \times 7 = 49$ combinations of α and β where $\alpha = \frac{1}{64}, \frac{1}{16}, \frac{1}{4}, 1, 4, 16, \text{and } 64$; $\beta = \frac{1}{64}, \frac{1}{16}, \frac{1}{4}, 1, 4, 16, \text{and } 64$.

571

572 Figure 5 Illustration of total cumulative viral load enlarged by mutations
573 producing strains of different antigen types. Each curve indicates the initial increase
574 followed by the decline in the number of cells infected by a strain of the same antigen
575 type, such as the one in Fig. 1(c). Arrows indicate mutations that result in mutants of
576 different antigen types. There are seven strains of different antigen types: a single strain
577 of the initial infection ($X_0 = 1$), three strains of the first-generation mutants ($X_1 = 3$);
578 two strains of the second-generation mutants ($X_2 = 2$); and one strain of the third-
579 generation mutant ($X_3 = 1$). The total cumulative viral load is 7φ. See text for
580 explanations.

581

582

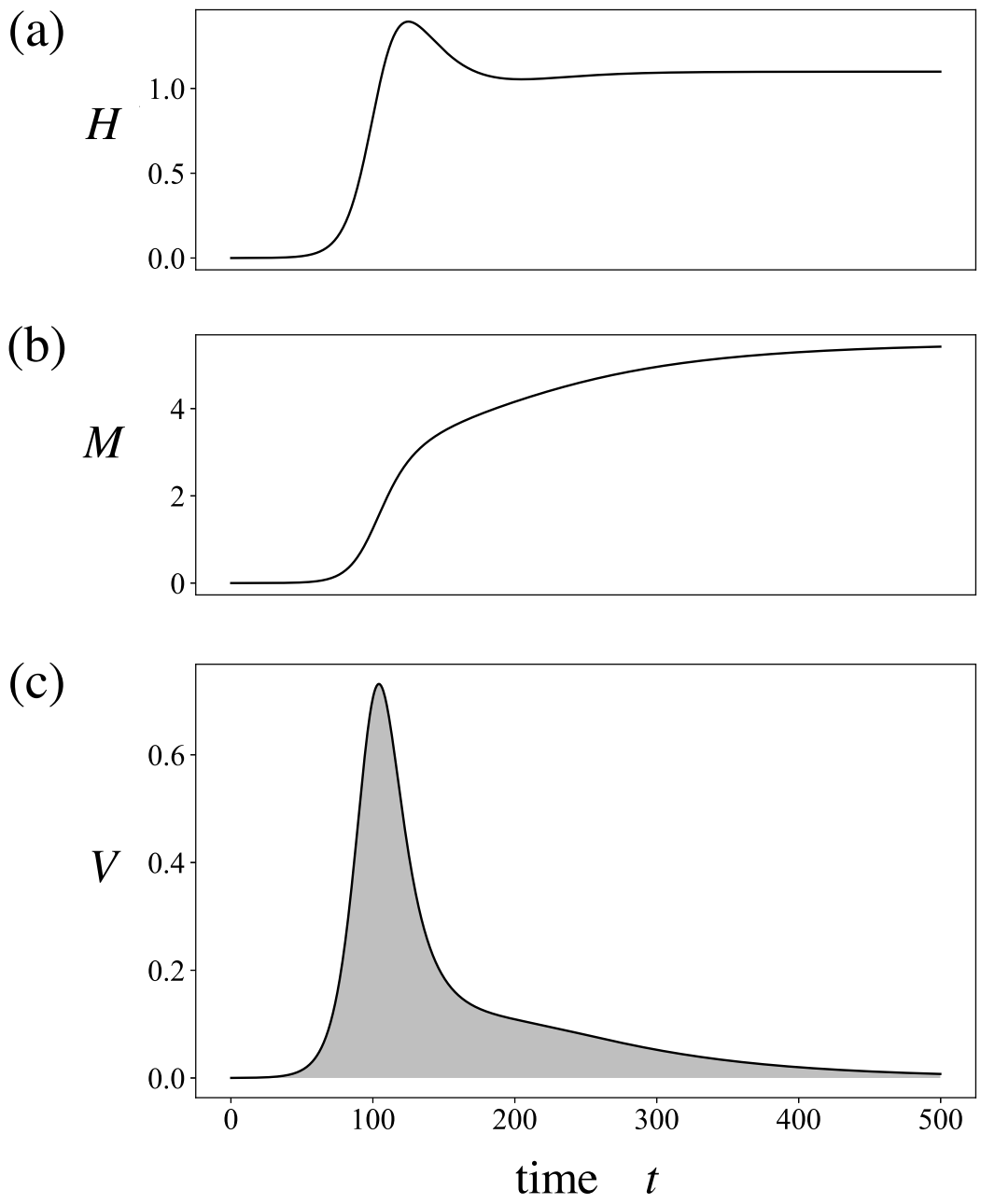
(a)
H
1.0
0.5
0.0
(b)
M
4
2
0
(c)
V
0.6
0.4
0.2
0.0
0
100
200
300
400
500
time t

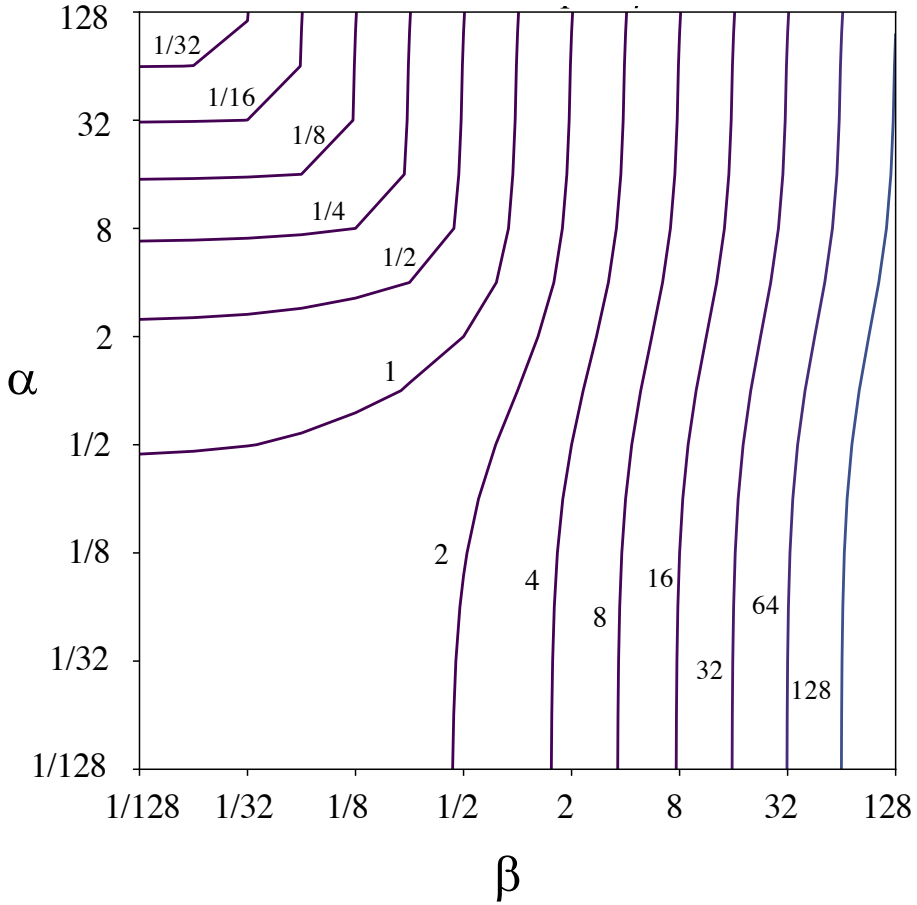
128
32
8
2
1/2
1/8
1/32
1/128
α
1/32
1/16
1/8
1/4
1/2
1
2
4
8
16
32
64
128
1/128
1/32
1/8
1/2
2
8
32
128
β

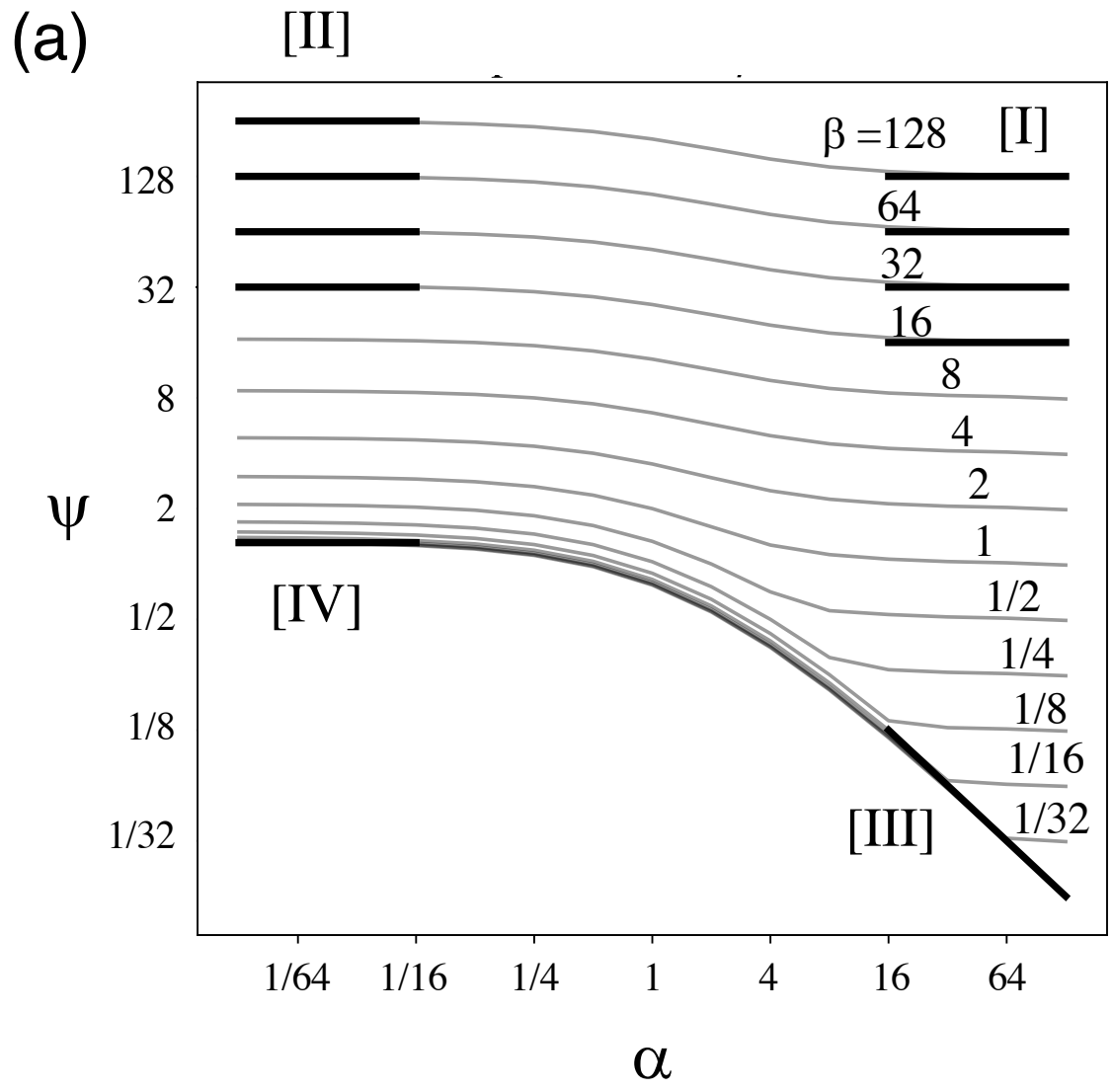
(a)
[II]
β =128
[I]
128
64
32
16
8
4
2
1
1/2
1/4
1/8
1/16
1/32
ψ
[IV]
[III]
1/64
1/16
1/4
1
4
16
64
α

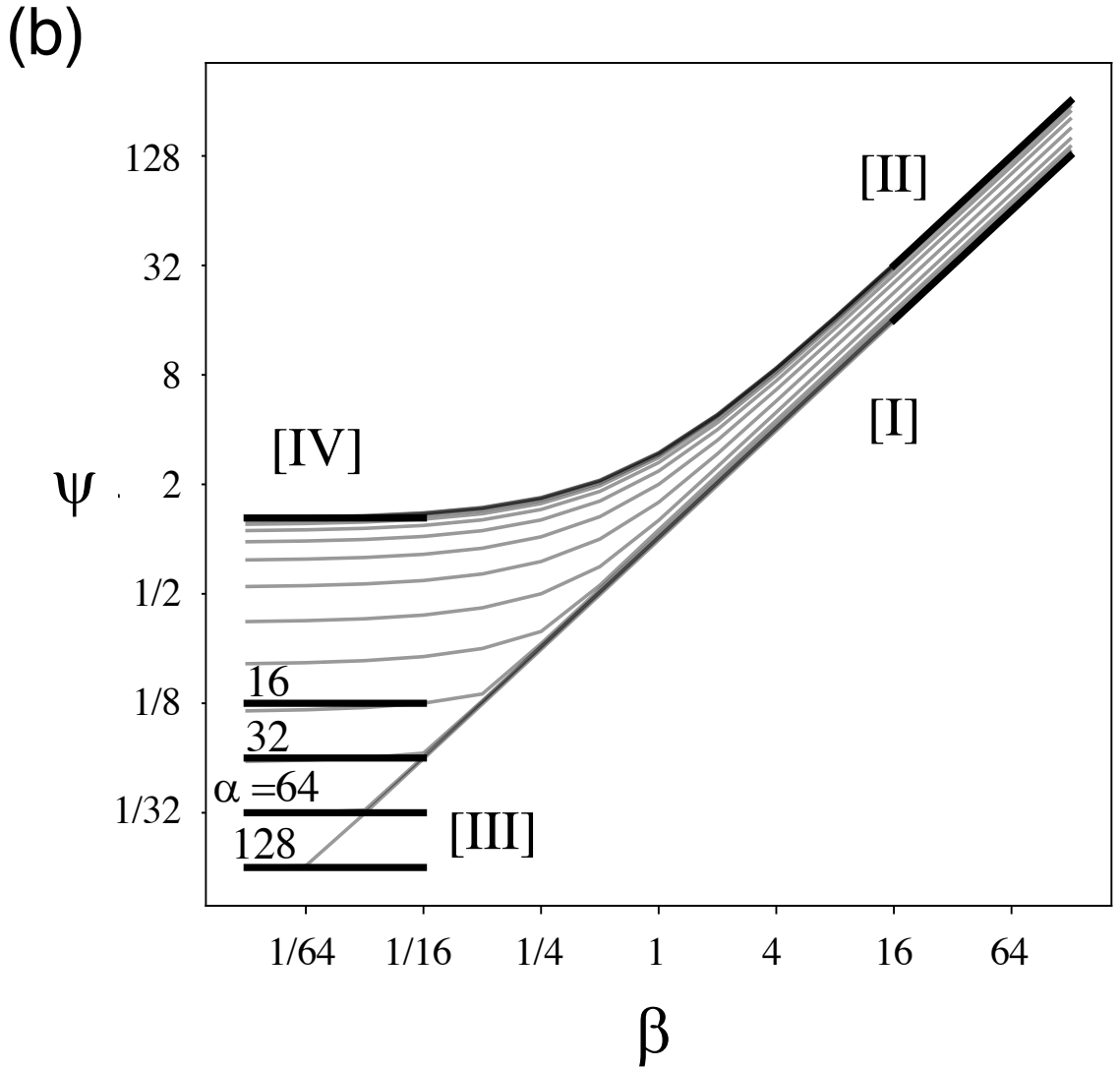
(b)
128
32
8
2
1/2
1/8
1/32
ψ
[II]
[I]
[IV]
16
32
α =64
128
[III]
1/64
1/16
1/4
1
4
16
64
β

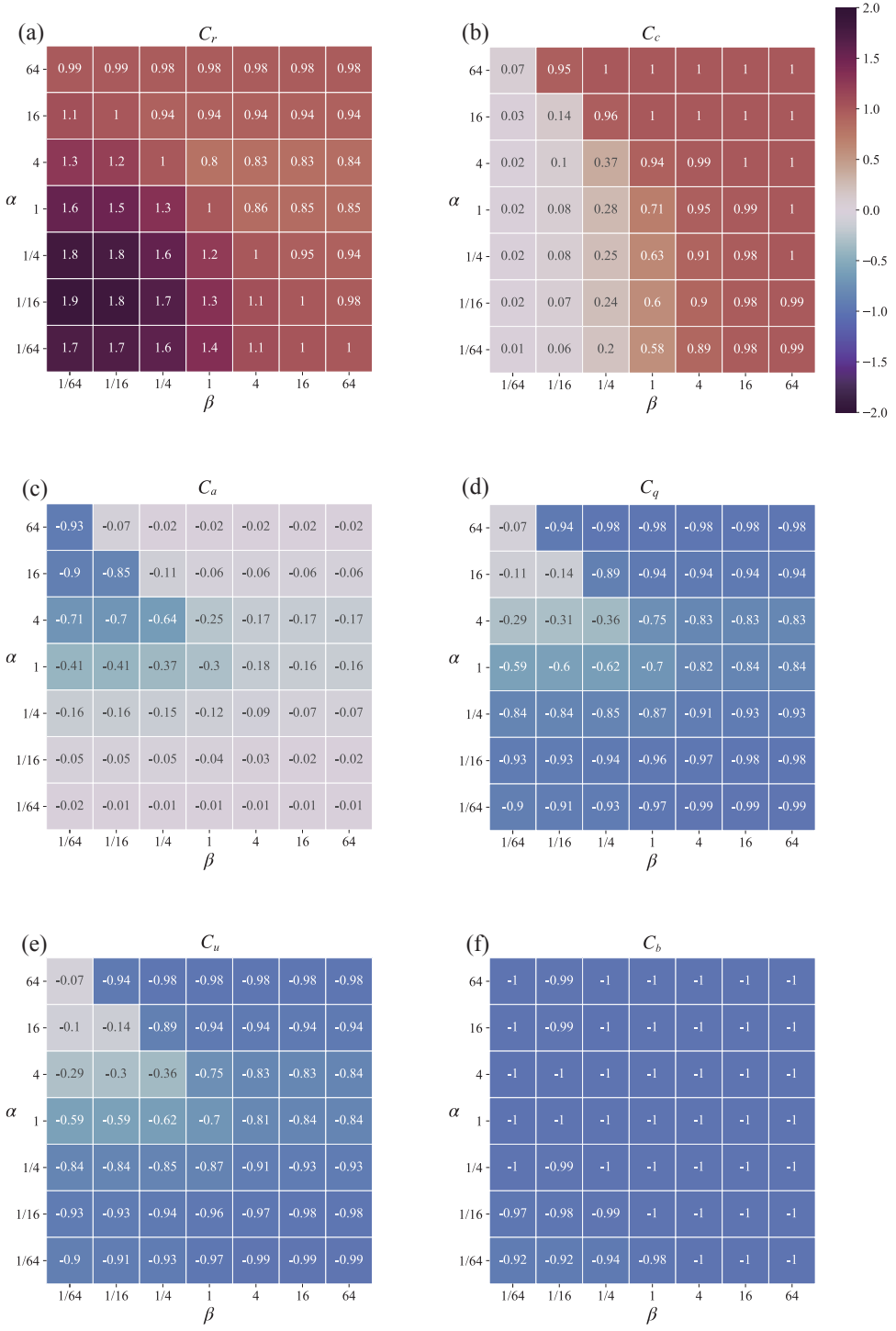
(a)
C_r
(b)
C_c
(c)
C_a
(d)
C_q
(e)
C_u
(f)
C_b
α
β
64
16
4
1
1/4
1/16
1/64
2.0
1.5
1.0
0.5
0.0
−0.5
−1.0
−1.5
−2.0

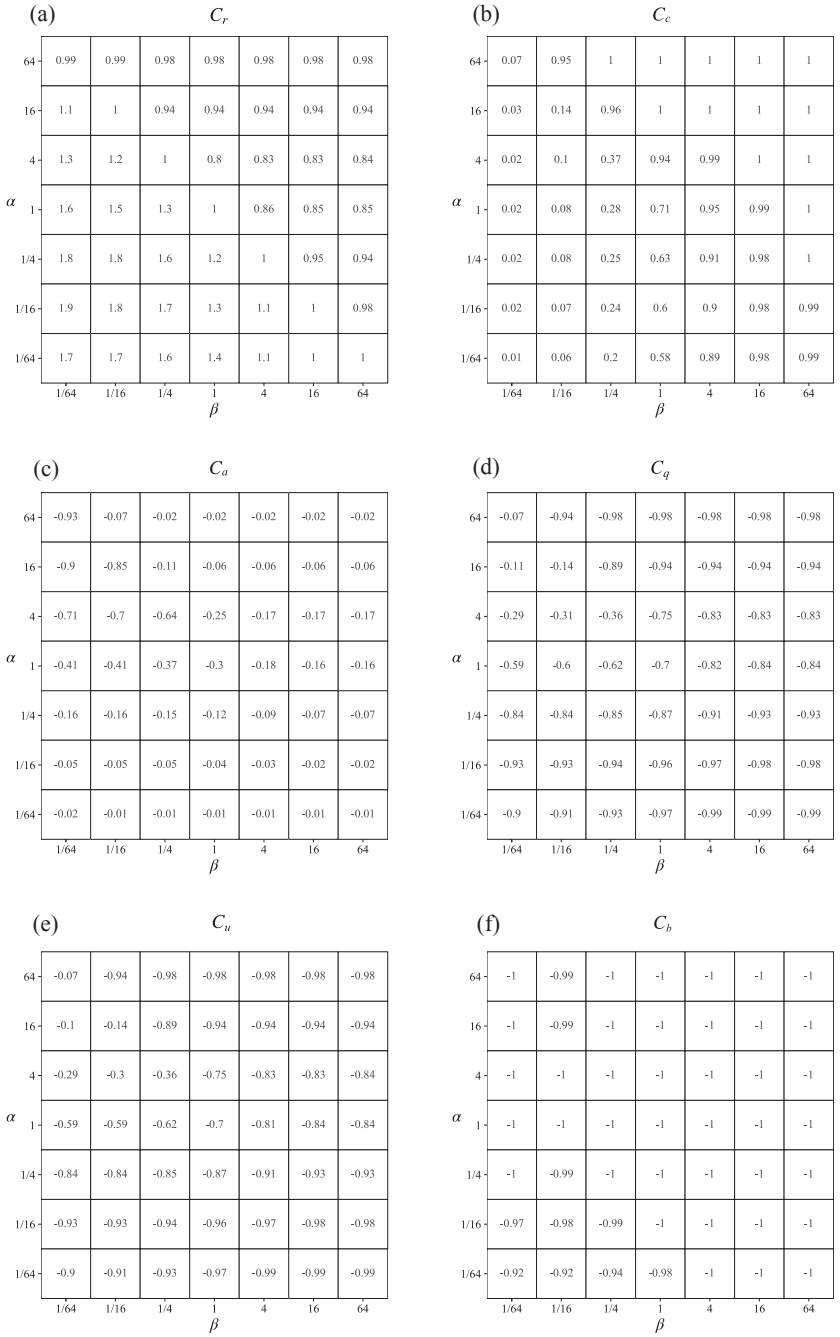
(a) C_r
64 0.99 0.99 0.98 0.98 0.98 0.98 0.98
16 1.1 1 0.94 0.94 0.94 0.94 0.94
4 1.3 1.2 1 0.8 0.83 0.83 0.84
α 1 1.6 1.5 1.3 1 0.86 0.85 0.85
1/4 1.8 1.8 1.6 1.2 1 0.95 0.94
1/16 1.9 1.8 1.7 1.3 1.1 1 0.98
1/64 1.7 1.7 1.6 1.4 1.1 1 1
1/64 1/16 1/4 1 4 16 64
β
(b) C_c
64 0.07 0.95 1 1 1 1 1
16 0.03 0.14 0.96 1 1 1 1
4 0.02 0.1 0.37 0.94 0.99 1 1
α 1 0.02 0.08 0.28 0.71 0.95 0.99 1
1/4 0.02 0.08 0.25 0.63 0.91 0.98 1
1/16 0.02 0.07 0.24 0.6 0.9 0.98 0.99
1/64 0.01 0.06 0.2 0.58 0.89 0.98 0.99
1/64 1/16 1/4 1 4 16 64
β
(c) C_a
64 -0.93 -0.07 -0.02 -0.02 -0.02 -0.02 -0.02
16 -0.9 -0.85 -0.11 -0.06 -0.06 -0.06 -0.06
4 -0.71 -0.7 -0.64 -0.25 -0.17 -0.17 -0.17
α 1 -0.41 -0.41 -0.37 -0.3 -0.18 -0.16 -0.16
1/4 -0.16 -0.16 -0.15 -0.12 -0.09 -0.07 -0.07
1/16 -0.05 -0.05 -0.05 -0.04 -0.03 -0.02 -0.02
1/64 -0.02 -0.01 -0.01 -0.01 -0.01 -0.01 -0.01
1/64 1/16 1/4 1 4 16 64
β
(d) C_q
64 -0.07 -0.94 -0.98 -0.98 -0.98 -0.98 -0.98
16 -0.11 -0.14 -0.89 -0.94 -0.94 -0.94 -0.94
4 -0.29 -0.31 -0.36 -0.75 -0.83 -0.83 -0.83
α 1 -0.59 -0.6 -0.62 -0.7 -0.82 -0.84 -0.84
1/4 -0.84 -0.84 -0.85 -0.87 -0.91 -0.93 -0.93
1/16 -0.93 -0.93 -0.94 -0.96 -0.97 -0.98 -0.98
1/64 -0.9 -0.91 -0.93 -0.97 -0.99 -0.99 -0.99
1/64 1/16 1/4 1 4 16 64
β
(e) C_u
64 -0.07 -0.94 -0.98 -0.98 -0.98 -0.98 -0.98
16 -0.1 -0.14 -0.89 -0.94 -0.94 -0.94 -0.94
4 -0.29 -0.3 -0.36 -0.75 -0.83 -0.83 -0.84
α 1 -0.59 -0.59 -0.62 -0.7 -0.81 -0.84 -0.84
1/4 -0.84 -0.84 -0.85 -0.87 -0.91 -0.93 -0.93
1/16 -0.93 -0.93 -0.94 -0.96 -0.97 -0.98 -0.98
1/64 -0.9 -0.91 -0.93 -0.97 -0.99 -0.99 -0.99
1/64 1/16 1/4 1 4 16 64
β
(f) C_b
64 -1 -0.99 -1 -1 -1 -1 -1
16 -1 -0.99 -1 -1 -1 -1 -1
4 -1 -1 -1 -1 -1 -1 -1
α 1 -1 -1 -1 -1 -1 -1 -1
1/4 -1 -0.99 -1 -1 -1 -1 -1
1/16 -0.97 -0.98 -0.99 -1 -1 -1 -1
1/64 -0.92 -0.92 -0.94 -0.98 -1 -1 -1
1/64 1/16 1/4 1 4 16 64
β

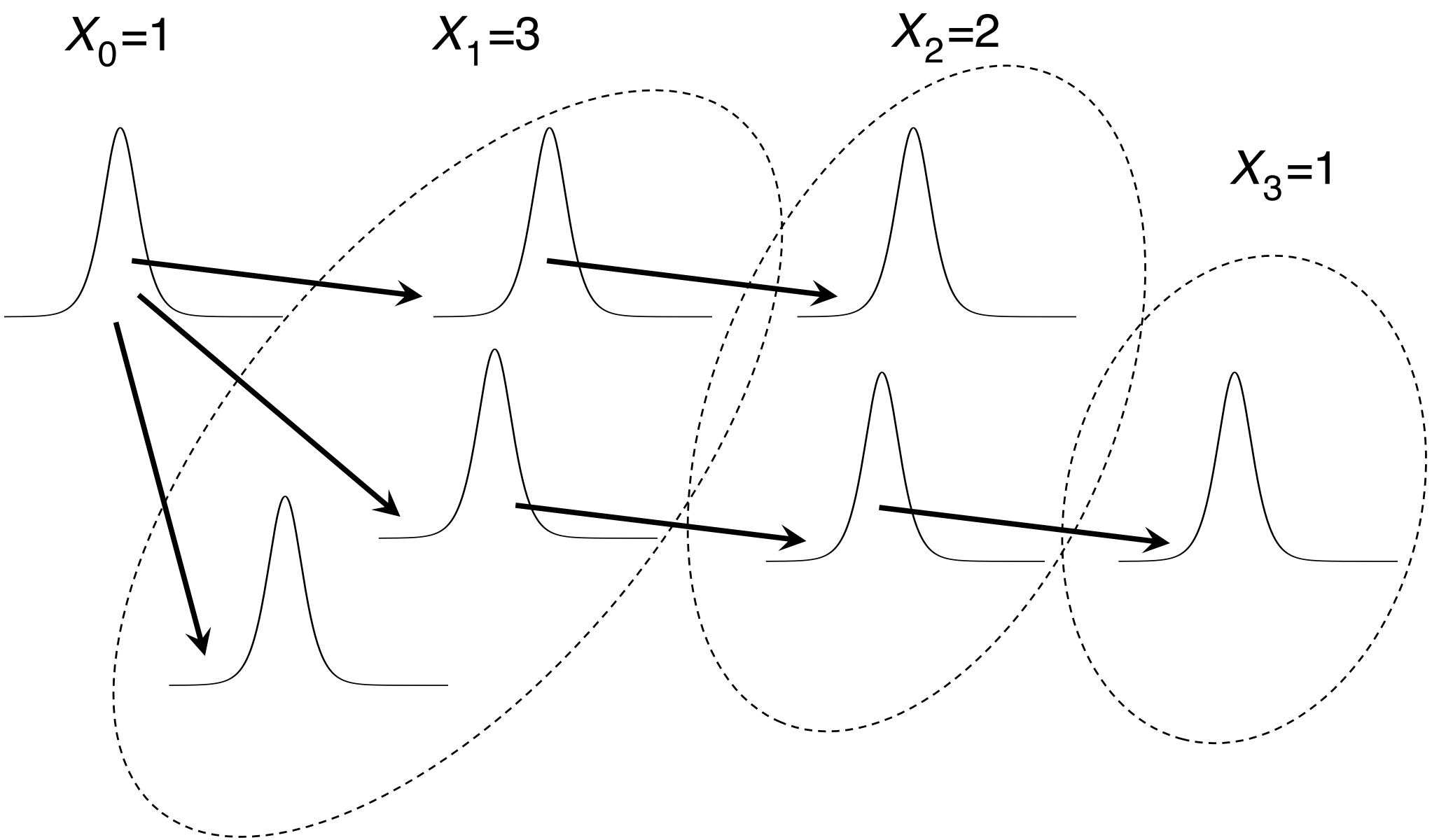
X_0=1
X_1=3
X_2=2
X_3=1

Figures

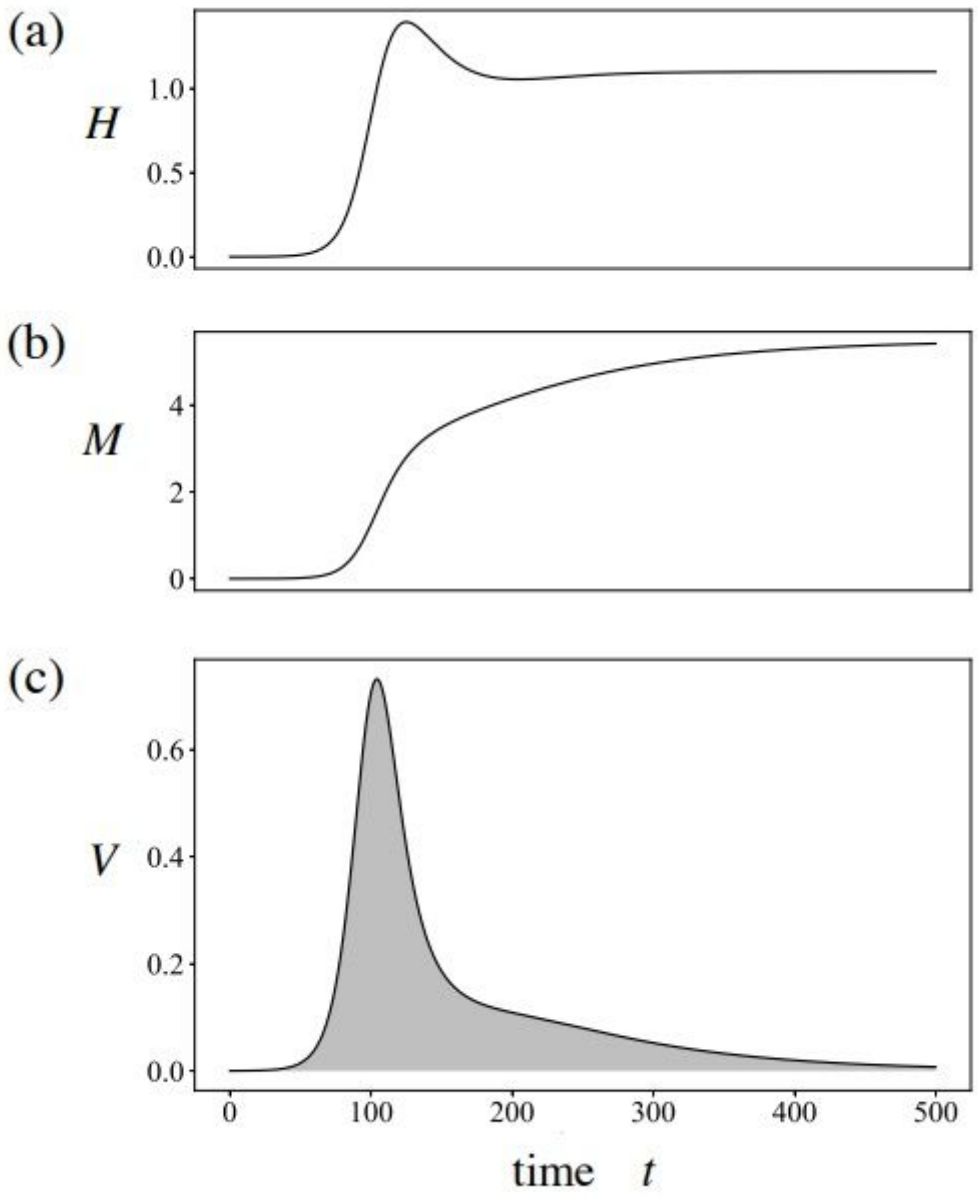

Figure 1

(see Manuscript file for caption)

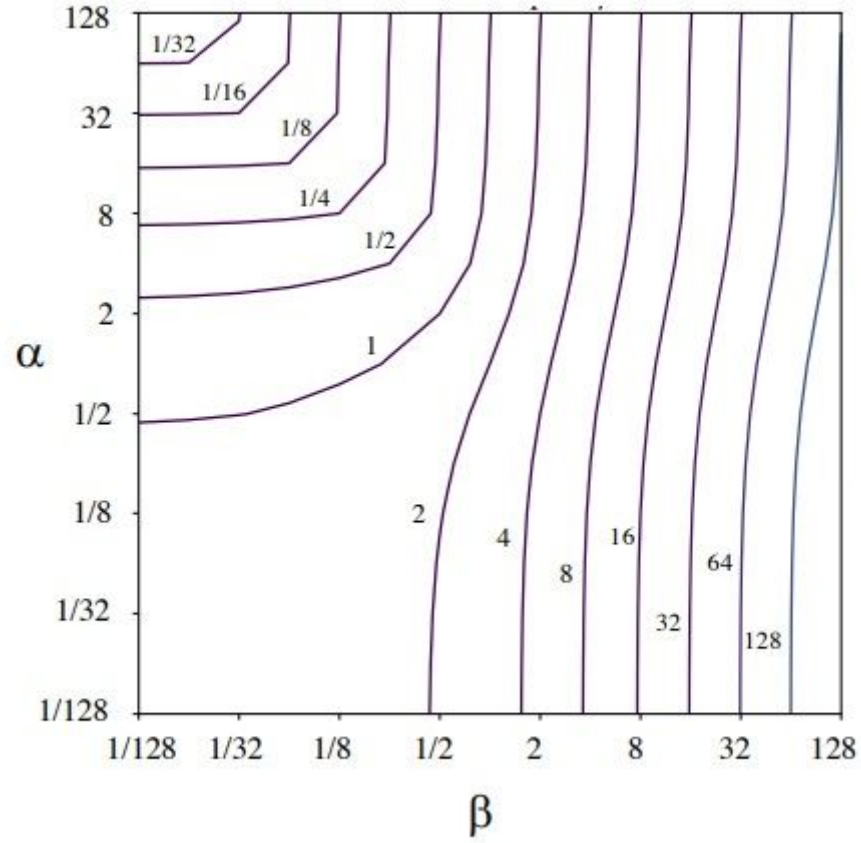

Figure 2

(see Manuscript file for caption)

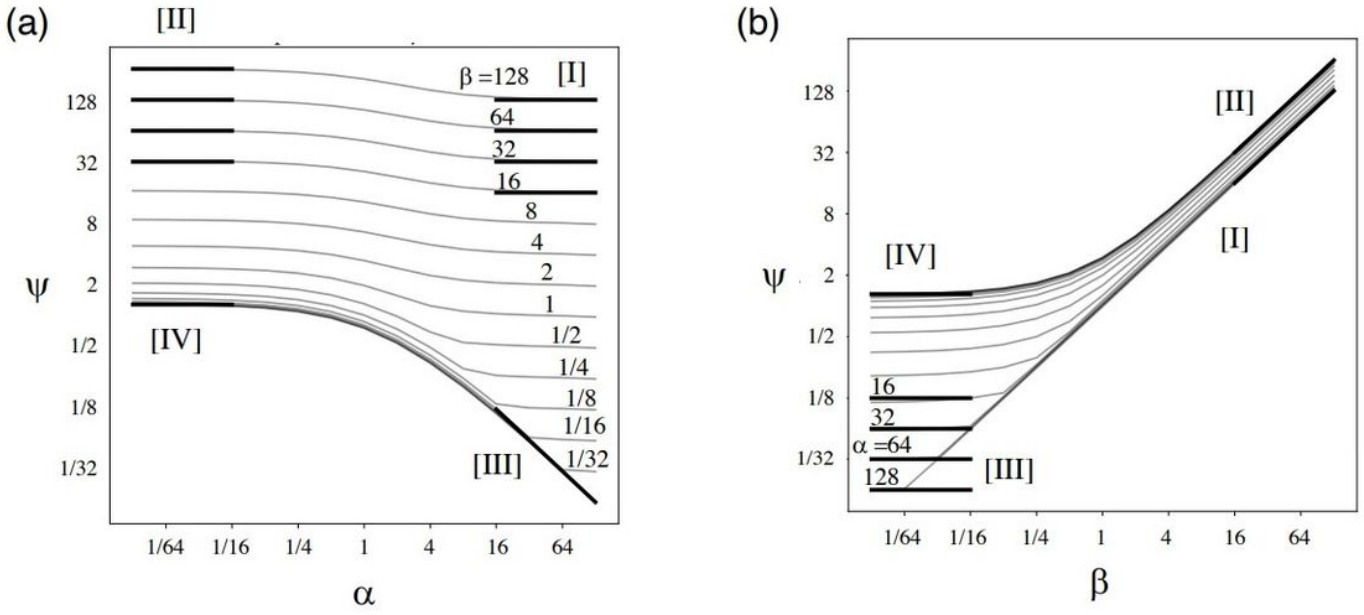

Figure 3

(see Manuscript file for caption)

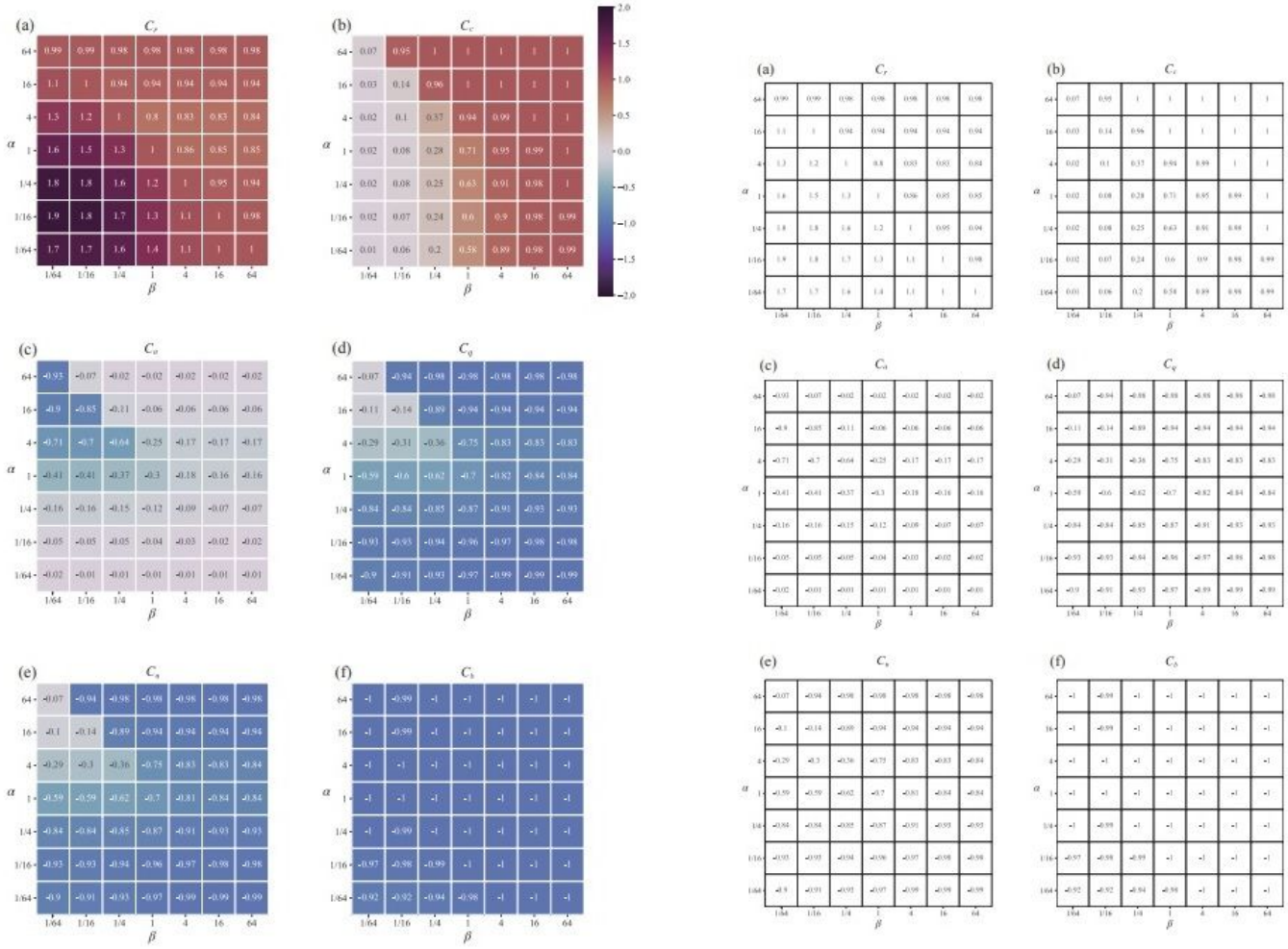

Figure 4

(see Manuscript file for caption)

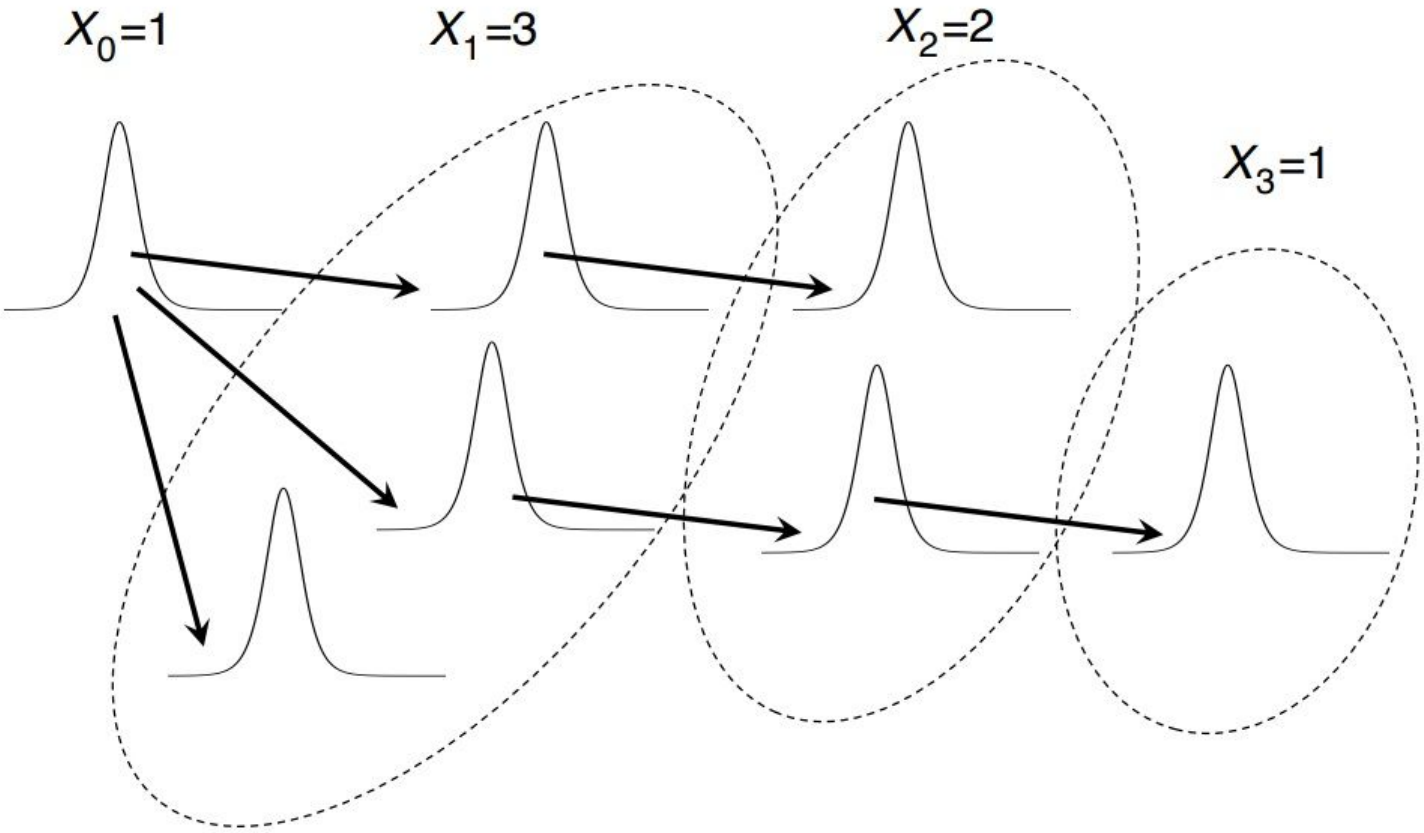

Figure 5

(see Manuscript file for caption)

Supplementary Files

This is a list of supplementary files associated with this preprint. Click to download.

- Iwasaetal.SIappendixes20210501YI.pdf